FM

NATIONAL AERONAUTICS AND SPACE ADMINISTRATION

MSC INTERNAL NOTE NO. 69-FM-224

August 12, 1969

Technical Library, Bellcomm, Inc.

FEB 9 1970

Internal Note No. 69-FM-224

SWITCHING LOGIC AND STEERING EQUATIONS FOR MULTIBURN EARTH ESCAPE MANEUVERS

FEB 74
RECEIVED
NASA STI FACILITY
INPUT BRANCH

Advanced Mission Design Branch

MISSION PLANNING AND ANALYSIS DIVISION

MANNED SPACECRAFT CENTER
HOUSTON, TEXAS

(NASA-TM-X-69774) SWITCHING LOGIC AND STEERING EQUATIONS FOR MULTIBURN EARTH ESCAPE MANEUVERS (NASA) 43 p

N74-70661

Unclas
00/99 16265

MSC INTERNAL NOTE NO. 69-FM-224

PROJECT APOLLO

SWITCHING LOGIC AND STEERING EQUATIONS FOR MULTIBURN EARTH ESCAPE MANEUVERS

By Jack Funk and Stewart F. McAdoo, Jr.
Advanced Mission Design Branch

August 12, 1969

MISSION PLANNING AND ANALYSIS DIVISION
NATIONAL AERONAUTICS AND SPACE ADMINISTRATION
MANNED SPACECRAFT CENTER
HOUSTON, TEXAS

Approved: Jack Funk
Jack Funk, Chief
Advanced Mission Design Branch

Approved: John P. Mayer
John P. Mayer, Chief
Mission Planning and Analysis Division

SWITCHING LOGIC AND STEERING EQUATIONS FOR MULTIBURN EARTH ESCAPE MANEUVERS

By Jack Funk and Stewart F. McAdoo, Jr.

1.0 SUMMARY

The use of multiburn-multiorbit maneuvers to inject spacecraft onto interplanetary missions significantly reduces gravity losses and thrust-to-weight-ratio requirements. Therefore, the application of this type of injection technique to manned interplanetary missions will increase performance and will reduce the cost of solid-core nuclear propulsion. Indispensable for the multiorbit injection technique is the development of engine switching logic and steering equations which will minimize gravity losses for the injection maneuvers. Derivations of near-optimum switching logic and steering equations are presented for the multiorbit injection technique with discussion and examples of the use of the technique.

The switching logic and steering equations are developed to minimize the difference between the velocity required for a single-impulse thrust maneuver and the velocity required for the multiorbit finite-thrust-maneuver. A loss function is developed which is a function of the characteristic velocity of the propulsion stage (or stages) and of the periapsis velocities of the multiorbit maneuver. It is shown geometrically that the finite-thrusting arcs are optimized if the engine is turned on when the derivative of the loss function is less than a constant value. The value of the derivative used to switch the thrust determines the number of injection orbits in the maneuver and the final escape velocity. The steering law used is derived by determination of the partial derivative of the total derivative of the loss function with respect to steering direction.

2.0 INTRODUCTION

The use of multiburn-multiorbit maneuvers for planetary escape (ref. 1) significantly reduces the gravity losses or thrust-to-weight requirements (or both) for escape maneuvers. The application of this type of injection technique to manned interplanetary missions will

considerably reduce cost if the primary propulsion is nuclear powered. Nuclear power will permit a considerable reduction in the required thrust level. The weight of a solid-core nuclear engine for a given thrust level is considerably greater than the weight of chemical propulsion systems. A typical engine mass fraction for nuclear propulsion is 0.2 of the thrust level. Therefore, a 75 000-pound-thrust engine will weight approximately 15 000 pounds. The increased weight and the cooldown fuel requirements for nuclear engines result in a significant performance penalty for high thrust levels.

Indispensable for the multiorbit escape maneuver is the development of engine switching logic and steering equations to optimize the maneuver. In this paper are presented the derivations of near-optimum switching logic and steering equations for a multiorbit escape maneuver with some discussion of their uses in mission guidance and control.

3.0 SYMBOLS

a	semimajor axis
$\dot{C}$	modified loss-function derivative
e	eccentricity
F	thrust
f	true anomaly
G	acceleration of gravity
K	switching constant
L	loss function
$\dot{L}$	time derivative of loss function
n	mean motion
p	semilatus rectum
q	effect of steering angle at time $t + \tau$
r	radius
T	total burn time

t time

V velocity

V_∞ hyperbolic excess velocity

ΔV impulsive velocity change

W weight

Z $$\frac{GF}{W} \frac{(t - \tau)(1 + e)}{eV_p\left[2 \frac{r_p}{r_{p,i}} - (1 - e)\right]}$$

α steering angle

β steering angle

γ flight-path angle

μ gravitational constant

τ time

Subscripts

a apoapsis

c characteristic

e equivalent

i initial

p periapsis

r radial

s horizontal

4.0 ANALYSIS

The multiorbit escape maneuver is illustrated in figure 1 which consists of a series of thrusting arcs separated by elliptical coasting arcs. The problem to be solved is development of a steering direction and a technique to determine when the engine should be started and stopped to minimize propulsion losses. Because propulsion loss is the function to be minimized, the first step is to write an equation for the propulsion losses.

4.1 Gravity Loss Function

The gravity losses are defined as the difference between the impulsive velocity change ΔV required for an impulsive escape maneuver with a specified hyperbolic excess velocity V_∞ and the characteristic velocity required to perform a maneuver to the same magnitude with finite thrust. The impulsive velocity change ΔV is the difference between the periapsis velocity V_p before and after the impulsive maneuver.

Because the periapsis radius may not be constant during a finite-thrust maneuver, a problem arises to define ΔV. This problem is solved by calculation of an equivalent periapsis velocity $V_{p,e}$ for the initial periapsis radius. A ΔV can be defined during the finite-thrust maneuver as the difference between the initial and the equivalent periapsis velocities. The equivalent periapsis velocity is calculated from the actual periapsis velocity by use of the relation

$$V_\infty^2 = V_p^2 - \frac{2\mu}{r_p} \tag{1}$$

where μ is the gravitational constant, r_p is the periapsis radius, and V_∞ is the hyperbolic excess velocity. The equivalent periapsis velocity is

$$V_{p,e} = \sqrt{V_p^2 - \frac{2\mu}{r_p} + \frac{2\mu}{r_{p,i}}} \tag{2}$$

The gravity losses during the finite-thrust maneuvers are calculated as follows.

$$L = V_c - \Delta V = \int_0^t \frac{GF}{W}\, d\tau - V_{p,e} + V_{p,i} \tag{3}$$

where G is the acceleration caused by gravity at surface, F is the rocket thrust, and W is the weight of the spacecraft.

4.2 Steering Equation

The steering equation is required to minimize the gravity loss during the thrusting arcs. The steering angle is defined as the angle that the thrust direction makes with the local horizontal. The angle is defined to be positive above the local horizontal and negative below the local horizontal. The symbol chosen for the thrust direction is β. It is necessary to find the function $\beta(t)$ which minimizes the loss L defined by the following.

$$L = \int_0^T \dot{L}\,(\beta(t),t)\, dt \tag{4}$$

where T is the total thrust time.

The rate of change of the gravity losses as a function of β and trajectory parameters is derived from equation (3) as

$$\dot{L} = \frac{GF}{W}\left[1 - \sqrt{\frac{1+e}{2\,\frac{r_p}{r_{p,i}} - (1-e)}}\;\frac{r_p}{r}\,(\cos\beta + \tan\gamma\,\sin\beta)\right] \tag{5}$$

The derivation is given in appendix A.

An interesting result is obtained when $\partial\dot{L}/\partial\beta$ is made equal to zero. Performance of this operation on $\dot{L}$ gives

$$\beta = \gamma \tag{6}$$

Thus, the often used approximation for the optimum steering direction along the velocity vector results from minimization of the time derivative of the gravity losses. This procedure is not a sufficient condition of an optimum because β at any given time has an effect not only at that time but at all subsequent times.

A clue to the effect of β on the gravity losses at time $t + \tau$ is obtained from the time history of $\dot{L}(\gamma,t)$ [fig. 2(a)]. The time derivative for a loss function L is shown for thrusting arcs which are constrained to pass through the same periapsis radius. It is seen that $\dot{L}$ goes to zero at all periapses. When thrusting occurs along the velocity vector $\dot{L}$ [fig. 2(b)] continually increases on each periapsis passage. The steering angle α that holds the periapsis constant [appendix B] is the following.

$$\alpha = \tan^{-1}\left[\left(\frac{r}{r_p} - 1\right)\frac{1}{\tan \gamma}\right] \tag{7}$$

This expression is indeterminate at $r = r_p$. After application of L'Hospital's rule, it is determined that $\alpha = 0$ at periapsis. Thus, the steering angle for both cases is zero at periapsis; however, the value of $\dot{L}$ is different. The cause for the difference is an accumulative effect of the steering function at periapsis which occurs before periapsis. This phenomenon suggests that the subsequent effect q of the steering direction at time $t + \tau$ can be approximated by evaluation of L for $r = r_p$ and $\beta = \gamma = 0$.

$$q = \frac{GF}{W}\left[1 - \sqrt{\frac{1 + e}{2\,\dfrac{r_p}{r_{p,i}} - (1 - e)}}\right] \tag{8}$$

A modified loss function is now constructed which consists of two parts. The first part $\dot{L} - q$ is the rate of change of the gravity losses caused by β at the current time. The second part is the estimate of the effect of the current steering direction on the loss function for the remaining thrust period. The function q is accumed to be monotonic at all times. Therefore, the total effect of $\beta(t)$ for the interval $T - t$ is given by the following integral.

$$\Delta L = \int_0^T \frac{dq}{dt} (T - t)\, d\tau \tag{9}$$

and

$$\frac{dq}{dt} = \frac{\partial q}{\partial r_p} \frac{dr_p}{dt} + \frac{\partial q}{\partial e} \frac{de}{dt} + \frac{\partial q}{\partial w} \frac{dw}{dt} \tag{10}$$

The modified loss function becomes the following.

$$\dot{C} = \dot{L} - q + \frac{dq}{dt} (T - t) \tag{11}$$

When $r_p/r_{p,i} = 1$ and $dq/dt = 0$, the condition for a constant periapsis radius $\dot{C} = \dot{L}$ occurs. The q represents the portion of the gravity losses caused by a change in periapsis radius from the initial value. A steering direction that minimizes the gravity losses can now be evaluated from the following equation

$$\frac{\partial \dot{C}}{\partial \beta} = 0 \tag{12}$$

and by use of the differential equations for changes in orbital elements caused by perturbing acceleration which were developed by Lagrange and given in reference 2. The derivation of the steering equation (appendix C), results in the following equation.

$$\beta = \tan^{-1} \left\{ \frac{\left[1 + Z \frac{r_p}{r_{p,i}} + Z\left(\frac{r_p}{r_{p,i}} - 1\right)\right] \tan \gamma}{\left[1 + Z \frac{r_p}{r_{p,i}} \left(1 - \frac{r^2}{r_p^2}\right) + Z\left(\frac{r_p}{r_{p,i}} - 1\right)\left(1 - \frac{r^2}{r_a r_p}\right)\right]} \right\} \tag{13}$$

Where

$$Z = \frac{GF}{W} \frac{(T - t)(1 + e)}{eV_p\left[2 \frac{r_p}{r_{p,i}} - (1 - e)\right]} \tag{14}$$

4.3 Switching Logic

The steering direction which minimizes the total effect of β on the gravity losses is given in equation (13). This effect is given by the modified loss function C. Because the modified loss function represents all the effects of $\beta(t)$ and none of the effects of β at other times, the following switching logic should minimize the gravity losses.

The multiorbit injection maneuver requires, in addition to the steering direction, a criterion for engine start and stop times. The criterion will have the capability to adjust the length of the various burns to minimize the gravity losses, subject to the constraint that the total burn time is a constant. The switching logic which accomplishes this task is stated as follows.

If thrusting is initiated when the derivative of the loss function is below a given value K and is stopped when the derivative of the loss function is above this same value K, then the resultant burn schedule will be optimum. The number of burns and the resultant end conditions will depend on the value of K. The proof that this switching logic does minimize the loss function is discussed geometrically with the aid of figure 3.

The optimum burn schedule is obtained when the engine is switched ON at point 1, OFF at point 2, ON at point 3, and OFF at point 4, and so forth. If the total burn time is constant for each burn and if the burn schedule is delayed for the first burn to ON at point 5 and OFF at point 6, the loss is reduced by the area under the cost function between points 1 and 5 and is increased by the area under the curve between points 2 and 6. Because the burn time is constant, the change in time Δt is the same for each increment. The increase in ΔV loss represented by the area between points 2 and 6 is greater than the decrease in ΔV loss represented by the area between points 1 and 5. An earlier start of the burn also results in an increase in the loss.

In the lower portion of figure 3, the effect of the relative length changes of burns 1 and 2 is illustrated. If burn 1 is shortened by turning the engine OFF at point 5 and if burn 2 is lengthened by turning the engine OFF at point 6 to keep the total burn time constant, then the decrease in the loss represented by the area between points 5 and 2 is less than the increase in the loss represented by the area between points 4 and 6.

A typical time history of $\dot{C}$ for a four-burn escape maneuver is shown in figure 4. Although the eccentricity of this orbit changes from near zero to greater than one, the $\dot{C}$-function for each burn is nearly identical to the previous burn. Thus, $\dot{C}$ is primarily a function of the position of the spacecraft with respect to the periapsis. The $\dot{C}$-function is almost totally unaffected by acceleration of the spacecraft. Therefore, the arguments for the optimality of the switching logic hold turn because perturbing the first burn by $\pm\Delta t$ will have the effect discussed previously.

5.0 DISCUSSION

An example of the characteristics of the steering equations for a four-burn multiorbit escape maneuver is shown in figures 4, 5, and 6. The time history of the steering direction compared to the flight-path angle is shown in figure 5, and a polar plot of the position of the thrusting arcs is shown in figure 6. Because the time history in figure 5 is shown as a function of engine burn time, the coasting arc of the trajectory is not shown. This example was calculated for an initial thrust-to-weight ration of 0.04 and a specific impulse of 825 seconds. These data represent a nuclear engine with 75 000 pounds of thrust which is pushing against 1 875 000 pounds of weight. The initial orbit for the example was elliptical with a 100-n. mi. perigee and a 400-n. mi. apogee. The equations are singular for an exact circular orbit. The terminal conditions for the escape maneuver are shown in table I.

Note the large differences between the flight-path angle and the thrust direction during the first burn. However, this difference is progressively reduced to zero at the end of the last burn. Examination of equation (13) indicates that the thrust direction will approach the flight-path angle as $T - t$ approaches zero. The effect of the large negative thrust direction in the early phases of the burn is a reduction in the rate of increase of the periapsis altitude in the early phases of the injection maneuver.

A comparison is shown in figure 5 between a calculus-of-variation solution for the thrust direction for a thrust maneuver between the initial orbit and the first intermidiate orbit and between the final intermediate orbit and the escape trajectory. The agreement is good between the calculus of variation and equation (13) as compared with thrust along the flight-path angle. It is difficult to make and conclusions with respect to the optimality of the techniques developed in this paper because the calculus-of-variation program used to determine the thrust direction on the first burn does not calculate optimum switching points for a multiorbit escape maneuver. However, the agreement shown between identical orbits is encouraging. The characteristic velocity V_c for the calculus-of-variation solution for the first burn was 2990 fps as compared to 3009 fps in table I.

From the space plots of the burn arcs shown in figure 6, is can be seen that each burn was started at approximately the same true anomaly. The shutdown points appear to be at different true anomalies because of a rotation of the periapsis position during the burn. The periapsis position was initialized to zero between each burn. The actual true anomalies at thrust ON and thrust OFF are shown in table I. Note that the ON and OFF commands are all within 1° of the same true anomaly angle except for the last command, in agreement with linear theory for a single burn which indicates that the optimum switching points should be at equal true anomalies on either side of periapsis.

Note from table I that the last orbit in the four-burn escape maneuver has a period of 8790 hours. In any practical mission plan, the switching logic would have to be perturbed from the optimum to limit the maximum period of the final orbit to some acceptable maximum such as 48 hours. For the example trajectory, it was desired to show the operation of the switching logic without such constraints. There is also a limit to the maximum escape velocity that can be obtained with a constant switching point. To obtain higher escape velocities, it is necessary to increase the magnitude of the switching constant for the final burn if the period of the last intermediate orbit is limited.

6.0 CONCLUSIONS

A quasi-optimum steering equation has been developed which is an expansion about the often used velocity-vector steering. A simple switching logic for calculation of multiburn earth escape maneuvers, the quasi-optimum steering equations, has been developed which optimizes the burn schedule. The magnitude of the switching function determines the number of burns and the final escape speed. The steering equation and switching logic should provide lower gravity losses than steering along the velocity vector, but no comparison has been made with a true optimum multiburn earth escape maneuver.

TABLE I.- PERFORMANCE FOR FOUR-BURN EARTH ESCAPE MANEUVER

Burn	V_p, fps	$V_{p,e}$, fps	Total V_c, fps	Total ΔV, fps	Total ΔV loss, fps	Initial true anomaly, deg	Final true anomaly, deg	h_p, n. mi.	h_a, n. mi.	Period, hr	V_∞, fps
Initial	26 082	26 082	0	0	0	--	--	100	400	1.56	--
1	28 355	28 741	3 009	2 659	349	-75	76.5	161	2 577	2.32	--
2	31 186	32 040	6 763	5 958	804	-76	75.0	252	9 357	5.22	--
3	34 787	36 131	11 449	10 049	1400	-75	74.8	379	2 328 019	8790	--
4	40 160	42 131	18 413	16 049	2364	-74	79	602	--	--	024

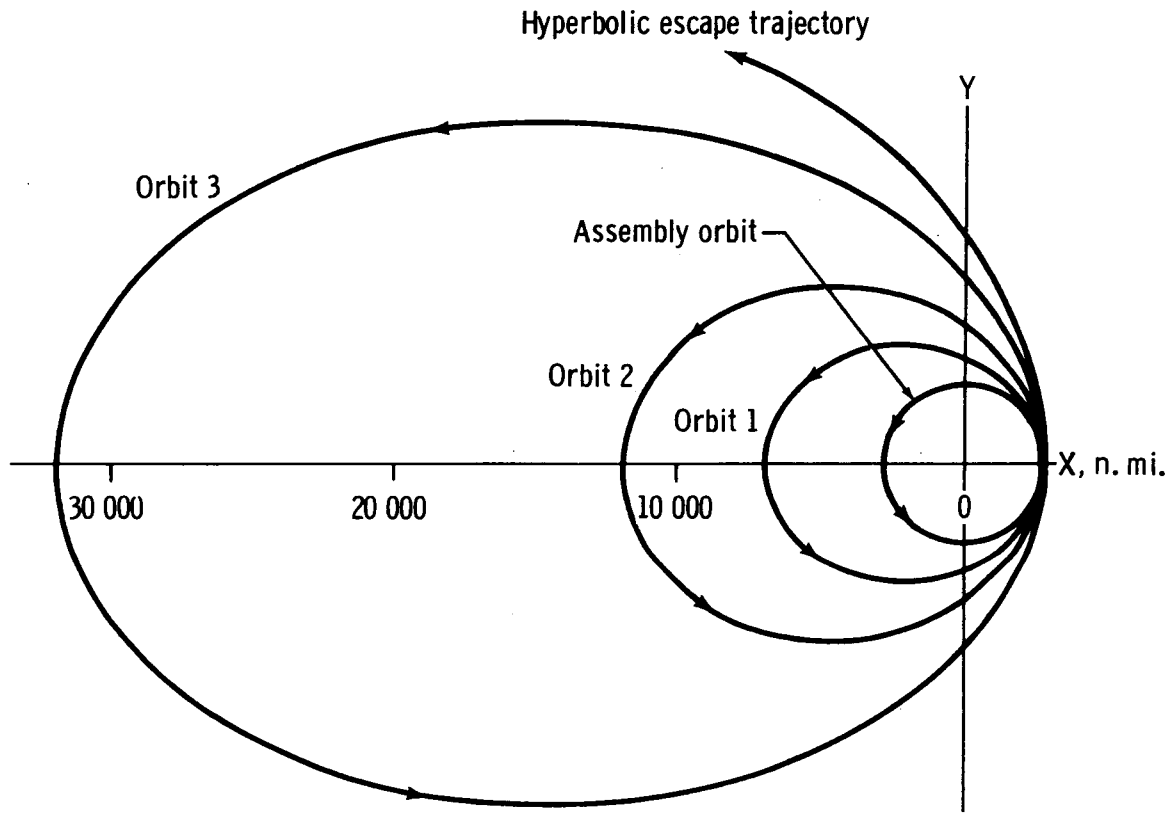

Figure 1. - Multiorbit injection profile for three orbits to escape.

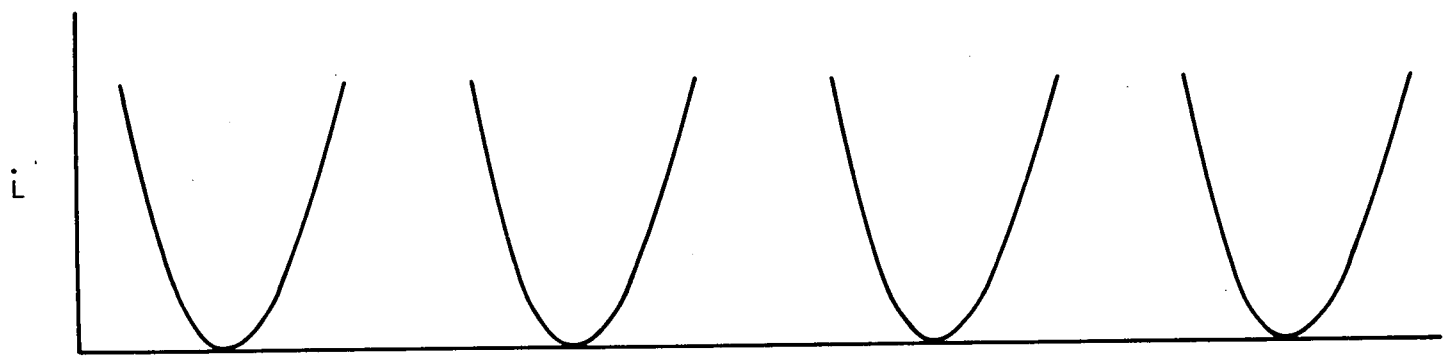

(a) Constrained thrusting.

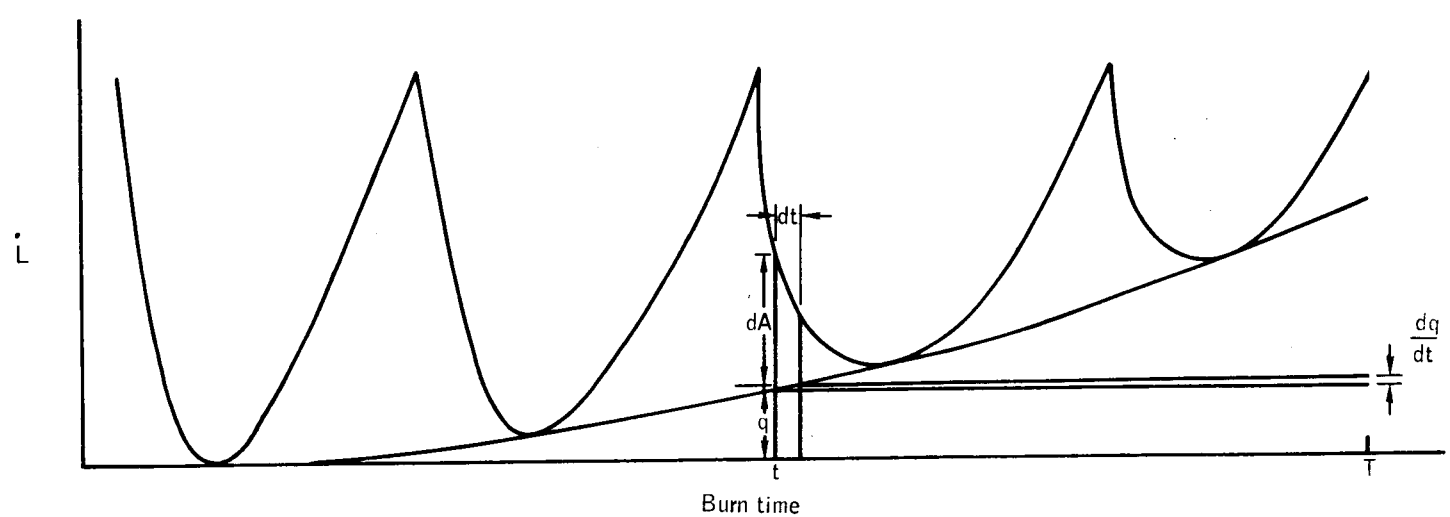

(b) Thrusting.

Figure 2.- Behavior of switching function, γ steering.

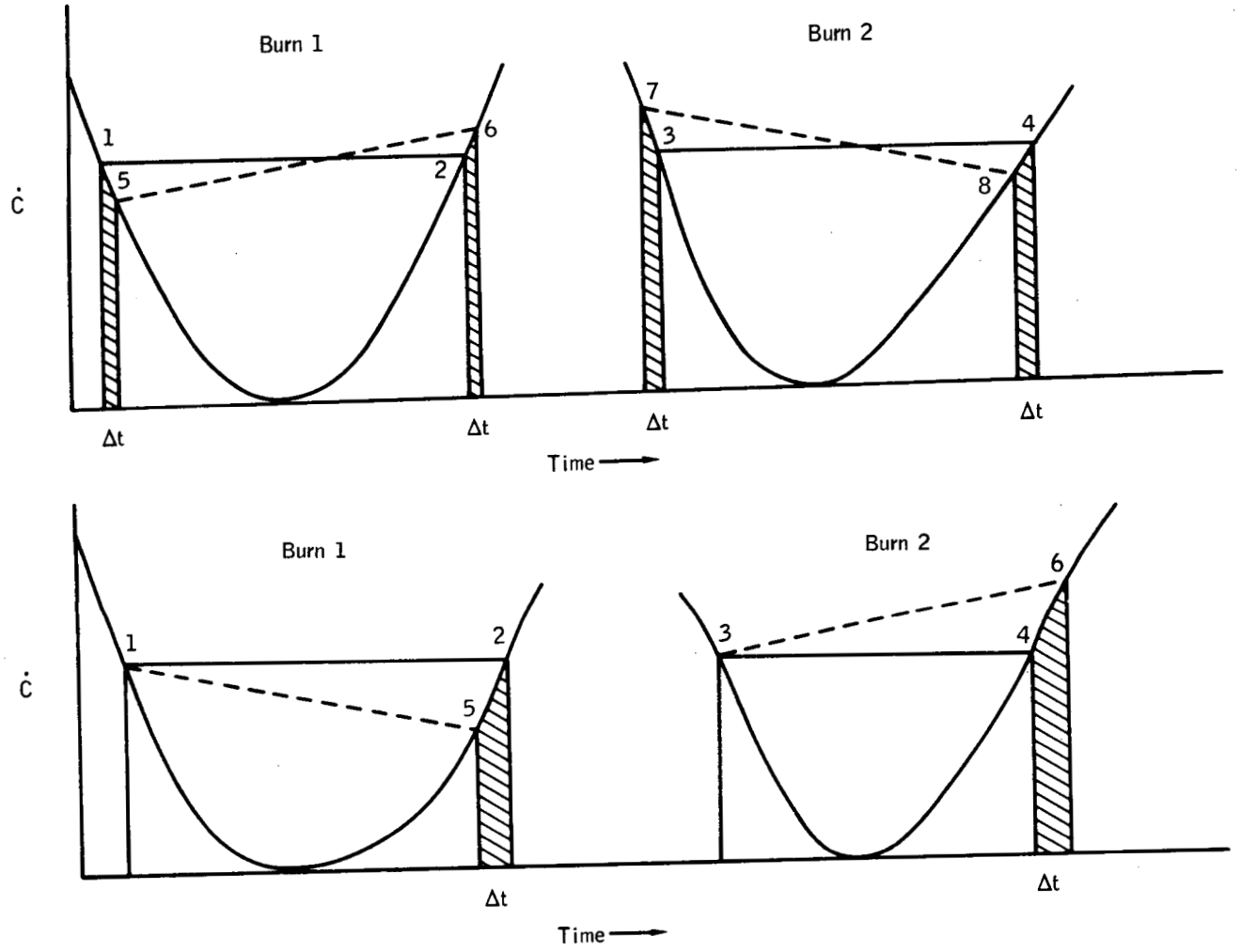

Figure 3.- Illustration of switching logic.

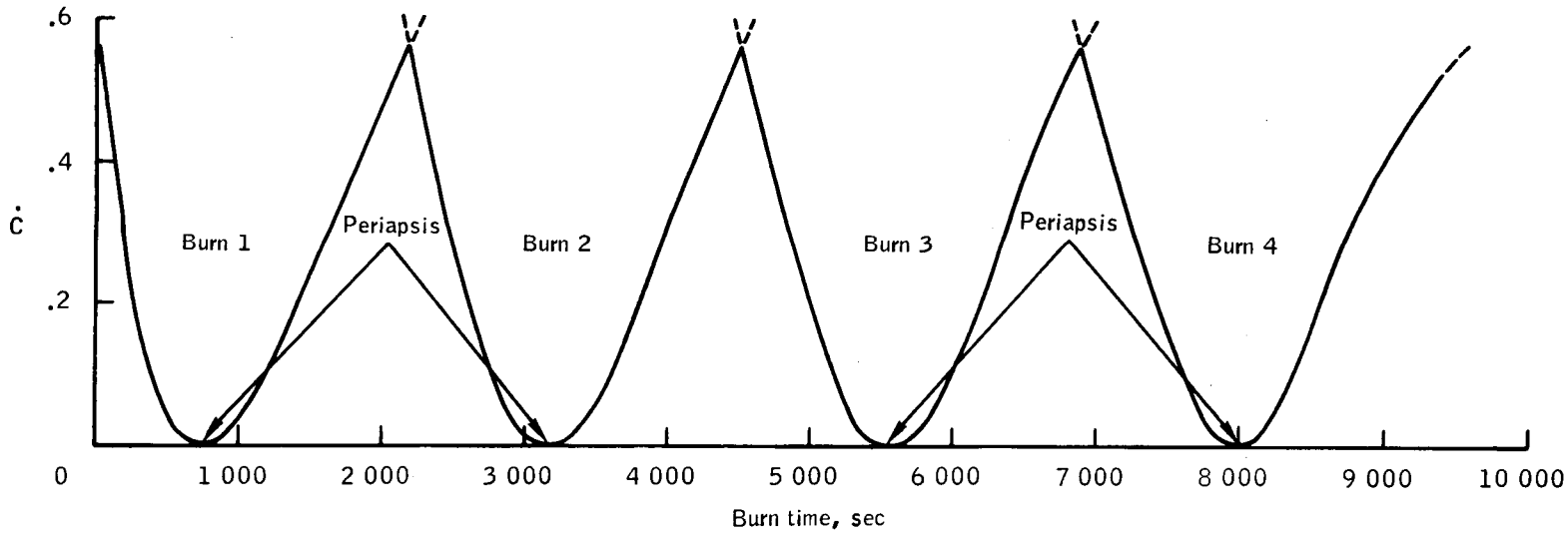

Figure 4.- Example of derivative of modified loss function for four-burn escape maneuver.

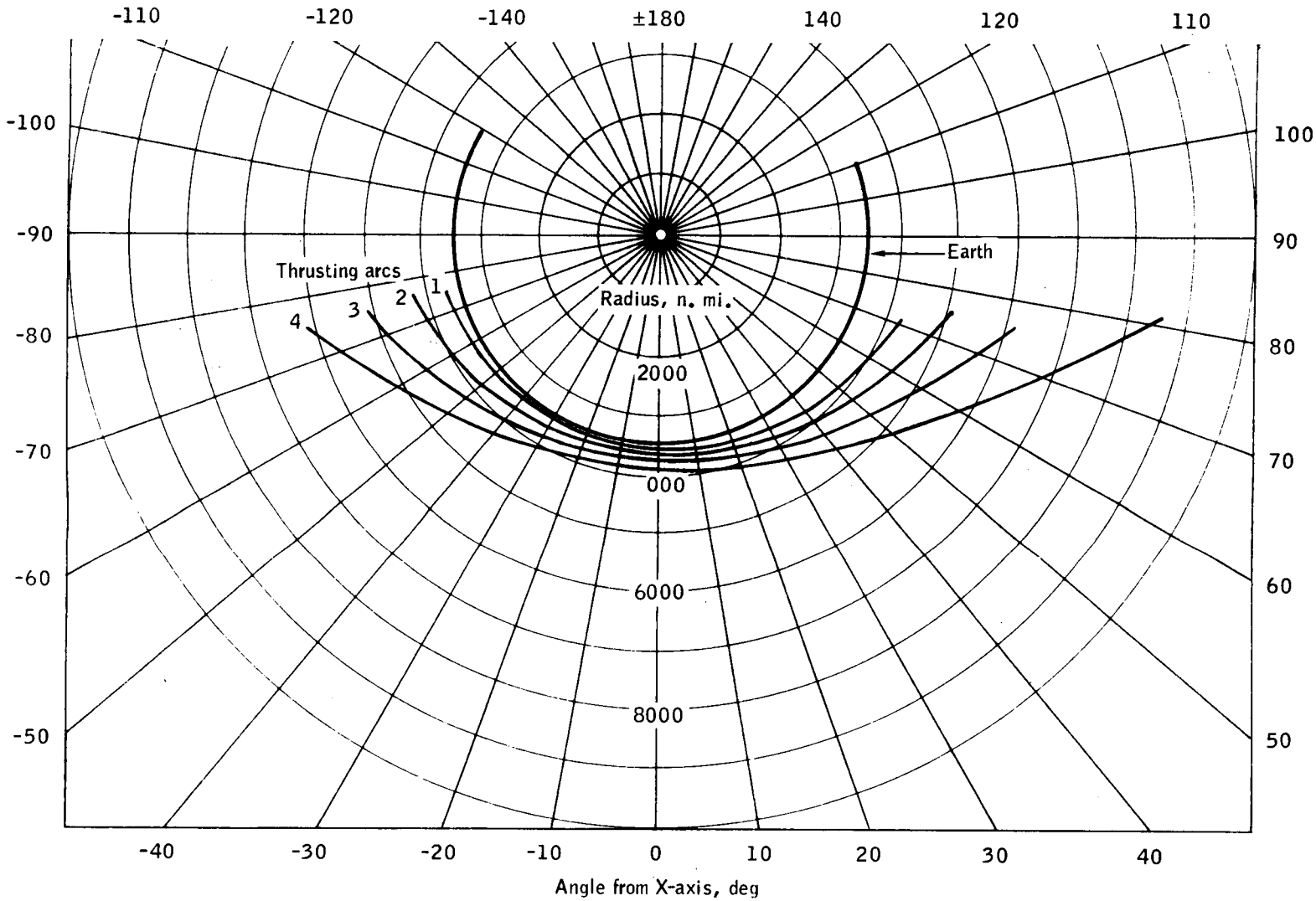

Figure 5.- Illustration of a 4-burn earth escape maneuver.

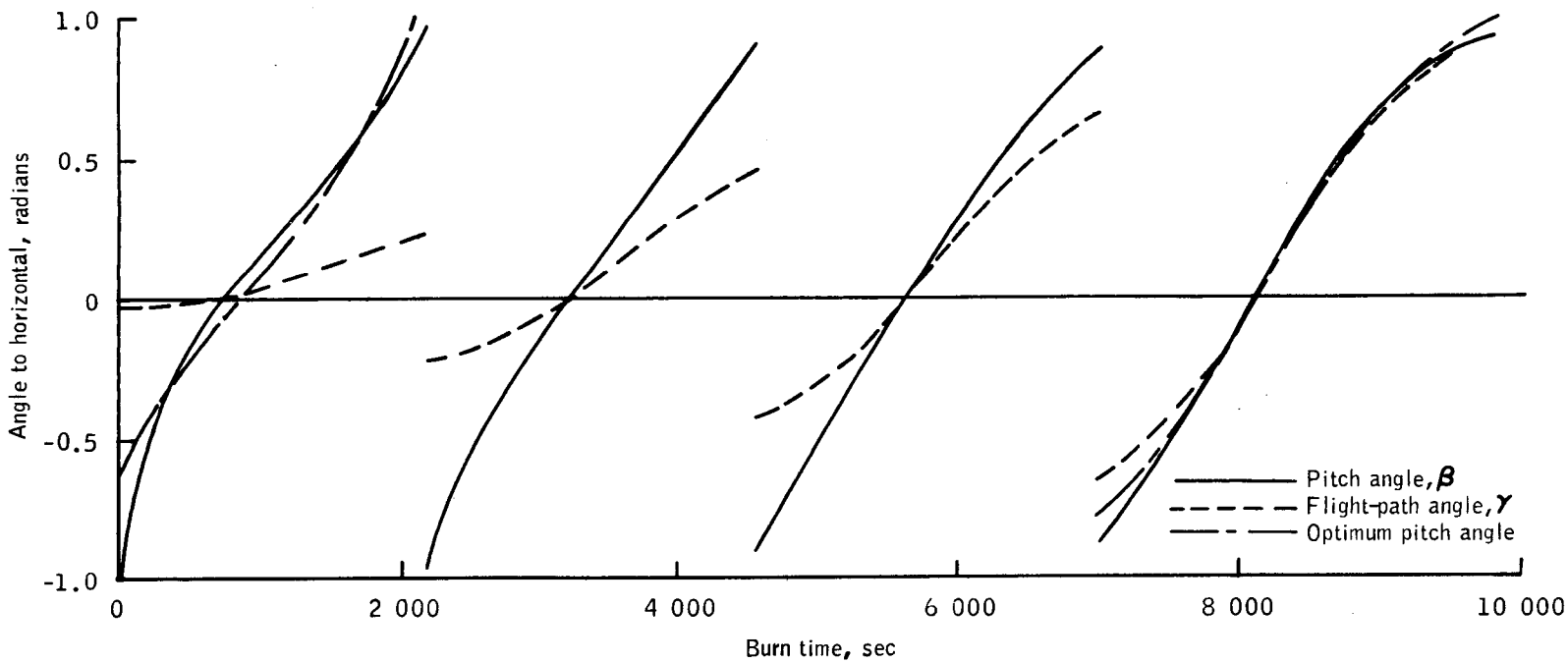

Figure 6.- Variation of thrust pitch angle with engine burn time.

APPENDIX A

DERIVATION OF dL/dt

APPENDIX A

DERIVATION OF dL/dt

From equation (4), the following were obtained.

$$L = \int_0^T \frac{GF}{W}\,dt - V_{p,e} + V_{p,i} \tag{A1}$$

$$\frac{d\dot{L}}{dt} = \frac{GF}{W} - \frac{dV_{p,e}}{dt} \tag{A2}$$

$$\dot{V}_{p,e} = \left(V_p^{\,2} - \frac{2\mu}{r_p} + \frac{2\mu}{r_{p,i}}\right)^{1/2} \tag{A3}$$

$$\frac{dV_{p,e}}{dt} = \frac{1}{2}\left(V_p^{\,2} - \frac{2\mu}{r_p} + \frac{2\mu}{r_{p,i}}\right)^{-1/2} \frac{d}{dt}\left(V_p^{\,2} - \frac{2\mu}{r_p} + \frac{2\mu}{r_{p,i}}\right) \tag{A4}$$

and

$$\frac{d}{dt}\left(V_p^{\,2} - \frac{2\mu}{r_p} + \frac{2\mu}{r_{p,i}}\right) = 2V_p\,\frac{dV_p}{dt} + \frac{2\mu}{r_p^{\,2}}\,\frac{dr_p}{dt} \tag{A5}$$

where V_p can be formed from the relations given in reference 3.

$$p = \frac{1}{\mu}(rV\cos\gamma)^2 \tag{A6}$$

$$V_p = \frac{\sqrt{\mu p}}{r_p} \tag{A7}$$

and

$$V_s = V \cos \gamma \tag{A8}$$

Then

$$V_p = \frac{rV \cos \gamma}{r_p} = \frac{r}{r_p} V_s \tag{A9}$$

$$\frac{dV_p}{dt} = \frac{r}{r_p} \frac{dV_s}{dt} + \frac{V_s}{r_p} \frac{dr}{dt} - \frac{rV_s}{r_p^2} \frac{dr_p}{dt} \tag{A10}$$

$$\frac{dr}{dt} = V \sin \gamma \tag{A11}$$

Acceleration in the horizontal direction caused by gravity is given by the subsequent relation

$$\frac{dV_s}{dt} = - \frac{V^2}{r} \cos \gamma \sin \gamma \tag{A12}$$

Addition of acceleration caused by the horizontal component of thrust F_s results in the following.

$$\frac{dV_s}{dt} = F_s - \frac{V^2}{r} \cos \gamma \sin \gamma \tag{A13}$$

Substitution of equations (A8), (A11), and (A13) into equation (A10) results in the following equations.

$$\frac{dV_p}{dt} = \frac{r}{r_p}\left(F_s - \frac{V^2}{r}\cos\gamma\sin\gamma\right)\frac{V^2}{r_p}\cos\gamma\sin\gamma - \frac{rV\cos\gamma}{r_p^{\,2}}\frac{dr_p}{dt}, \tag{A14}$$

$$\frac{dV_p}{dt} = \frac{r}{r_p}F_s - \frac{rV\cos\gamma}{r_p^{\,2}}\frac{dr_p}{dt} \tag{A15}$$

Substitution of equation (A15) into equation (A5) yields

$$\begin{aligned}\frac{dV_{p,e}}{dt} &= \frac{1}{2}\left(V_p^{\,2} - \frac{2\mu}{r_p} + \frac{2\mu}{r_{p,i}}\right)^{-1/2}\left[2V_p\left(\frac{r}{r_p}F_s - \frac{rV\cos\gamma}{r_p^{\,2}}\frac{dr_p}{dt}\right) + \frac{2\mu}{r_p^{\,2}}\frac{dr_p}{dt}\right] \\ &= \frac{1}{2}\left(V_p^{\,2} - \frac{2\mu}{r_p} + \frac{2\mu}{r_{p,i}}\right)^{-1/2}\left[\frac{2V_p r}{r_p}F_s - \left(\frac{2rVV_p}{r_p^{\,2}}\cos\gamma - \frac{2\mu}{r_p^{\,2}}\right)\frac{dr_p}{dt}\right]\end{aligned} \tag{A16}$$

By substitution of two-body orbital relationships and simplification, equation (A17) is obtained.

$$\frac{dV_{p,e}}{dt} = \frac{1}{2}\left(V_p^{\,2} - \frac{2\mu}{r_p} + \frac{2\mu}{r_{p,i}}\right)^{-1/2}\left(\frac{2V_r r}{r_p}F_s - \frac{2\mu e}{r_p^{\,2}}\frac{dr_p}{dt}\right) \tag{17}$$

To find dr_p/dt, the two-body relationship given in reference 4 is differentiated.

$$r_p = a(1 - e) \tag{A18}$$

$$\frac{dr_p}{dt} = (1 - e)\frac{da}{dt} - a\frac{de}{dt} \tag{A19}$$

The derivatives da/dt and de/dt are given in reference 2 as the following.

$$\frac{da}{dt} = \frac{2}{nr\sqrt{1 - e^2}}\left[erF \sin f + a\left(1 - e^2\right) F_s\right] \tag{A20}$$

$$\frac{de}{dt} = \frac{\sqrt{1 - e^2}}{nae}\left\{eF_r \sin f + \left[\frac{a\left(1 - e^2\right)}{r} - \frac{r}{a}\right]F_s\right\} \tag{A21}$$

After substitution of equation (A21) into equation (A19) and simplification by use of conic relationships found in reference 3, equation (A22) results.

$$\frac{dr_p}{dt} = \frac{r_p^{\,2}(1 + e)}{V_p re}\left[-F_r \tan \gamma + \left(\frac{r^2}{r_p^{\,2}} - 1\right)F_s\right] \tag{A22}$$

The components of thrusting F_r and F_s are

$$F_r = \frac{GF}{W} \sin \beta \qquad F_s = \frac{GF}{W} \cos \beta \tag{A23}$$

$$\frac{dr_p}{dt} = \frac{GF}{W} \frac{r_p^{\,2}(1 + e)}{V_p re} \left[-\tan \gamma \sin \beta + \left(\frac{r^2}{r_p^{\,2}} - 1 \right) \cos \beta \right] \tag{A24}$$

Substitution of equation (A24) into equation (A17) and simplification result in equation (A25)

$$\frac{dV_{p,e}}{dt} = \sqrt{\frac{1 + e}{2 \frac{r_p}{r_{p,i}} - (1 - e)}} \left(\frac{r_p}{r} \cos \beta + \frac{r_p}{r} \tan \gamma \sin \beta \right) \tag{A25}$$

When $\frac{dV_{p,e}}{dt}$ in equation (A1) is replaced, equation (A26) results.

$$\dot{L} = \frac{dL}{dt} = \frac{GF}{W} \left[1 - \frac{r_p}{r} \sqrt{\frac{1 + e}{2 \frac{r_p}{r_{p,i}} - (1 - e)}} (\cos \beta + \tan \gamma \sin \beta) \right] \tag{A26}$$

APPENDIX B

DETERMINATION OF THRUSTING DIRECTION FOR A STEERING EQUATION

APPENDIX B

DETERMINATION OF THRUSTING DIRECTION FOR A STEERING EQUATION

The solution of the equation

$$\frac{dr_p}{dt} = 0 \tag{B1}$$

for the thrusting direction α for a steering equation is needed. To develop equation (B1) into a steering equation, use is made of several equations that are based on a two-body spherical solution to the equation of motion.

$$r_p = a(1 - e) \tag{B2}$$

and

$$\frac{dr_p}{dt} = (1 - e)\frac{da}{dt} - a\frac{de}{dt} \tag{B3}$$

as given in reference 2.

$$\frac{da}{dt} = \frac{2}{nr\sqrt{1 - e^2}}\left[erF_r \sin f + a\left(1 - e^2\right)F_s\right] \tag{B4}$$

$$\frac{de}{dt} = \frac{\sqrt{1 - e^2}}{nae}\left\{eF_r \sin f + \left[\frac{a\left(1 - e^2\right)}{r} + \frac{r}{a}\right]F_s\right\} \tag{B5}$$

Substitution of equations (B4) and (B5) into equation (B3) and the collecting of terms results in the following equation

$$\frac{dr_p}{dt} = -F_r \sin f - \frac{1}{e}\left[\frac{a\left(1 - e^2\right)}{r} - \frac{r}{a}\right] F_s = 0 \tag{B6}$$

With equation (B2)

$$\frac{F_r}{F_s} = \frac{1 + e}{\sin f}\left(\frac{r^2 - r_p^{\,2}}{err_p}\right) \tag{B7}$$

The angle of the thrust vector with respect to the horizontal is

$$\tan \alpha = \frac{F_r}{F_s} = \frac{1 + e}{\sin f}\left(\frac{r^2 - r_p^{\,2}}{err_p}\right) \tag{B8}$$

The angle α is equal to zero when the force is at right angles to the radius and positive clockwise. Therefore, -90° is thrusting along the radius toward the planet, and 0° is at right angles to the radius in the direction of motion. Equation (B8) represents the steering logic used in the performance analysis. Another form of equation (B8) is obtained by substitution of the relation

$$\sin f = \frac{a\left(1 - e^2\right)\tan \gamma}{er} \tag{B9}$$

into equation (B8)

$$\tan \alpha = \frac{r^2 - r_p^{\,2}}{a r_p (1 - e) \tan \gamma} = \left(\frac{r^2}{r_p^{\,2}} - 1 \right) \frac{1}{\tan \gamma} \tag{B10}$$

This form is more convenient in digital calculations because $\tan \gamma$ is easily computed from the position and velocity

APPENDIX C

DETERMINATION OF THE STEERING ANGLE

APPENDIX C

DETERMINATION OF THE STEERING ANGLE

The loss function $\dot{C}$ is given in equation (11) as the following

$$\dot{C} = \dot{L} + \left(\frac{\partial q}{\partial r_p}\frac{dr_p}{dt} + \frac{\partial q}{\partial e}\frac{de}{dt} + \frac{\partial q}{\partial W}\frac{dW}{dt}\right)(T - t) - q \tag{C1}$$

The solution of the equation

$$\frac{\partial \dot{C}}{\partial \beta} = 0 \tag{C2}$$

for β is needed; therefore

$$\frac{\partial \dot{C}}{\partial \beta} = \frac{\partial \dot{L}}{\partial \beta} + \left[\frac{\partial q}{\partial r_p}\left(\frac{\partial}{\partial \beta}\frac{dr_p}{dt}\right) + \frac{dr_p}{dt}\left(\frac{\partial}{\partial \beta}\frac{\partial q}{\partial r_p}\right) + \frac{\partial q}{\partial \beta}\left(\frac{\partial}{\partial \beta}\frac{de}{dt}\right) + \frac{de}{dt}\left(\frac{\partial}{\partial \beta}\frac{\partial q}{\partial e}\right)\right.$$
$$\left. + \frac{\partial q}{\partial W}\left(\frac{\partial}{\partial \beta}\frac{\partial W}{\partial t}\right) + \frac{dW}{dt}\left(\frac{\partial}{\partial \beta}\frac{\partial q}{\partial W}\right)\right](T - t) - \frac{\partial q}{\partial \beta} \tag{C3}$$

Note by inspection of equation (8) that

$$\frac{\partial}{\partial \beta}\frac{\partial q}{\partial r_p} = \frac{\partial}{\partial \beta}\frac{\partial q}{\partial e} = \frac{\partial}{\partial \beta}\frac{\partial q}{\partial W} = \frac{\partial q}{\partial \beta} = 0 \tag{C4}$$

Equation (C3) is then

$$\frac{\partial \dot{C}}{\partial \beta} = \frac{\partial \dot{L}}{\partial \beta} + \left[\frac{\partial q}{\partial r_p}\left(\frac{\partial}{\partial \beta}\frac{dr_p}{dt}\right) + \frac{\partial q}{\partial e}\left(\frac{\partial}{\partial \beta}\frac{de}{dt}\right)\right](T - t) \tag{C5}$$

As given in equation (5)

$$\dot{L} = \frac{GF}{W}\left[1 - \sqrt{\frac{1 + e}{2\frac{r_p}{r_{p,i}} - (1 - e)}}\left(\frac{r_p}{r}\cos\beta + \frac{r_p}{r}\tan\gamma\sin\beta\right)\right] \tag{C6}$$

therefore

$$\frac{\partial \dot{L}}{\partial \beta} = \frac{GF}{W}\frac{r_p}{r}\sqrt{\frac{1 + e}{2\frac{r_p}{r_{p,i}} - (1 - e)}}(\sin\beta - \tan\gamma\cos\beta) \tag{C7}$$

The derivatives $\partial q/\partial r_p$ and $\partial q/\partial e$ are

$$\frac{\partial q}{\partial r_p} = \frac{GF}{W}(T - t_1)\frac{\sqrt{1 + e}}{r_{p,i}\left[2\frac{r_p}{r_{p,i}} - (1 - e)\right]^{3/2}} \tag{C8}$$

$$\frac{\partial q}{\partial e} = -\frac{GF}{W}(T - t_1)\frac{r_p - r_{p,i}}{r_{p,i}\sqrt{1 + e}\left[2\frac{r_p}{r_{p,i}} - (1 - e)\right]^{3/2}} \tag{C9}$$

In appendix A, dr_p/dt is derived as

$$\frac{dr_p}{dt} = \frac{r_p^{\,2}(1 + e)}{V_p re} \frac{GF}{W} \left[-\tan \gamma \sin \beta + \left(\frac{r^2}{r_p^{\,2}} - 1 \right) \cos \beta \right] \tag{C10}$$

therefore

$$\frac{\partial}{\partial \beta} \frac{dr_p}{dt} = \frac{GF}{W} \frac{r_p^{\,2}(1 + e)}{V_p re} \left[\left(1 - \frac{r^2}{r_p^{\,2}} \right) \sin \beta - \tan \gamma \cos \beta \right] \tag{C11}$$

In reference 2, de/dt is given as

$$\frac{de}{dt} = \frac{\sqrt{1 - e^2}}{r_a e} \left\{ eF_r \sin f + \left[\frac{a\left(1 - e^2\right)}{r} - \frac{r}{a} \right] F_2 \right\} \tag{C12}$$

By simplification

$$\frac{de}{dt} = \frac{GF}{W} \frac{a\left(1 - e^2\right)}{er} \sqrt{\frac{r_p(1 + e)}{\mu}} \left[\tan \gamma \sin \beta + \left(1 - \frac{r^2}{a^2\left(1 - e^2\right)} \right) \cos \beta \right] \tag{C13}$$

so that

$$\frac{\partial}{\partial\beta}\frac{de}{dt} = \frac{GF}{W}\frac{a\left(1 - e^2\right)}{er}\sqrt{\frac{r_p(1 + e)}{\mu}}\left\{\left[\frac{r^2}{a^2\left(1 - e^2\right)} - 1\right]\sin\beta + \tan\gamma\cos\beta\right\} \quad (C14)$$

The required partial derivative having been computed, $\partial\dot{C}/\partial\beta$ becomes

$$\frac{\partial\dot{C}}{\partial\beta} = \frac{GF}{W}\frac{r_p}{r}\sqrt{\frac{1 + e}{2\frac{r_p}{r_{p,i}} - (1 - e)}}\,(\sin\beta - \tan\gamma\cos\beta)$$

$$+ \frac{GF}{W}(T - t)\frac{\sqrt{1 + e}}{r_{p,i}\left[2\frac{r_p}{r_{p,i}} - (1 - e)\right]^{3/2}}\left\{\frac{GF}{W}\frac{r_p^{\,2}(1 + e)}{V_p re}\left[\left(1 - \frac{r^2}{r_p^{\,2}}\right)\sin\beta - \tan\gamma\cos\beta\right]\right\}$$

$$- \frac{GF}{W}(T - t)\frac{r_p - r_{p,i}}{r_{p,i}\sqrt{1 + e}\left[2\frac{r_p}{r_{p,i}} - (1 - e)\right]^{3/2}}\left[\frac{GF}{W}\frac{a\left(1 - e^2\right)}{er}\sqrt{\frac{r_p(1 + e)}{\mu}}\left\{\left[\frac{r^2}{a^2\left(1 - e^2\right)} - 1\right]\sin\beta + \tan\gamma\cos\beta\right\}\right] \quad (C15)$$

By equating $\partial c/\partial\beta$ to zero and dividing out terms with the substitutions of equations (C7), (C8), (C9), (C10), and (C14)

$$0 = \sin\beta - \tan\gamma\cos\beta$$

$$+ \frac{GF}{W}\frac{(T - t)(1 + e)}{eV_p\left(Z\dfrac{r_p}{r_{p,i}} - (1 - e)\right)}\frac{r_p}{r_{p,i}}\left[\left(1 - \frac{r^2}{r_p^2}\right)\sin\beta - \tan\gamma\cos\beta\right] \tag{C16}$$

$$+ \frac{GF}{W}\frac{(T - t)(1 + e)}{eV_p\left(2\dfrac{r_p}{r_{p,i}} - (1 - e)\right)}\left(\frac{r_p}{r_{p,i}} - 1\right)\left[\left(1 - \frac{r^2}{r_a r_p}\right)\sin\beta - \tan\gamma\cos\beta\right]$$

Define

$$Z = \frac{GF}{W}\frac{(T - t)(1 + e)}{eV_p\left(2\dfrac{r_p}{r_{p,i}} - (1 - e)\right)} \tag{C17}$$

Then by substituting and collecting terms

$$\left[1 + Z\frac{r_p}{r_{p,i}}\left(1 - \frac{r^2}{r_p^2}\right) + Z\left(\frac{r_p}{r_{p,i}} - 1\right)\left(1 - \frac{r^2}{r_a r_p}\right)\right]\sin\beta$$

$$= \left[1 + Z\frac{r_p}{r_{p,i}} + Z\left(\frac{r_p}{r_{p,i}} - 1\right)\right]\tan\gamma\cos\beta \tag{C18}$$

or

$$\beta = \tan^{-1}\left\{\frac{\left[1 + Z\frac{r_p}{r_{p,i}} + Z\left(\frac{r_p}{r_{p,i}} - 1\right)\right]\tan\gamma}{\left[1 + Z\frac{r_p}{r_{p,i}}\left(1 - \frac{r^2}{r_p^{\,2}}\right) + Z\left(\frac{r_p}{r_{p,i}} - 1\right)\left(1 - \frac{r^2}{r_a r_p}\right)\right]}\right\} \tag{C19}$$

REFERENCES

1. Johnson, P. G.; and Rom, F. E.: Perigee Propulsion for Orbital Launch of Nuclear Rockets. NASA TR R-140, 1962.

2. Blanco, V. M.; and McCuskey, S. W.: Basic Physics of the Solar System. Addison-Wesley Publishing Co., 1961.

3. Jensen, J.; Townsend, G.; Kork, J.; and Kraft, D.: Design Guide to Orbital Flight. McGraw-Hill Book Co., Inc., 1962.

4. Ehricke, Kraft A.: Space Flight. D. Van Nostrand Co., Inc., 1960.